JACS
JOURNAL OF THE AMERICAN CHEMICAL SOCIETY
pubs.acs.org/JACS
Article

Electron Affinity of UF_6

Burak A. Tufekci, Shiying Wang, Lan Cheng,* and Kit H. Bowen*

Cite This: https://doi.org/10.1021/jacs.6c08451
Read Online
ACCESS | Metrics & More | Article Recommendations | Supporting Information

ABSTRACT: We report an anion photoelectron spectroscopic study of the photodetachment of uranium hexafluoride anion (UF_6^-) to neutral UF_6, the primary species involved in uranium isotopic enrichment. The adiabatic electron affinity (AEA) of UF_6 and the vertical detachment energy (VDE) of UF_6^-, both predicted using high-level relativistic coupled-cluster calculations, provided unequivocal support for the assignment of the observed spectral features in the anion photoelectron spectrum of UF_6^-. The experimental AEA value of UF_6 and the VDE value of UF_6^- were determined to be 5.05 ± 0.10 eV and 5.66 ± 0.10 eV, respectively. This work provides the first direct, spectroscopic determination of the electron affinity of UF_6.

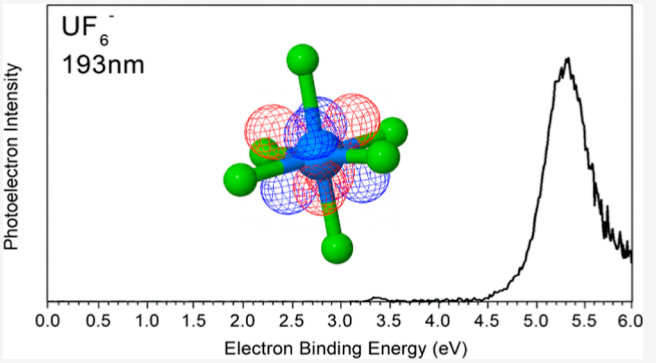

INTRODUCTION

Uranium hexafluoride (UF_6) has been central to nuclear technology since the 1940s,[1] especially as a *sine qua non* of the uranium enrichment process.[2−4] Due to its volatility, it garnered fame for being the uranium-containing compound used for isotopic enrichment in the gaseous diffusion process of the Manhattan Project.[5] More recently, UF_6 has become central to the centrifugal isotope separation process. The selective excitation of UF_6 has also been explored as a potential route for laser-based isotope separation.[6−11] Beyond its technological significance, UF_6 and its ions have long attracted attention in the chemical physics community with gas-phase experiments yielding fundamental molecular insight via electronic and vibrational spectroscopy.[12−19] Furthermore, the potential multiple-bonding[20] character of UF_6 is ostensibly due to the participation of 5f electrons in chemical bonding, a central focus in heavy element and relativistic quantum chemistry.[21−24]

While numerous theoretical studies of the electronic structure of UF_6 and its ions have been conducted, experimental validation has remained incomplete. Key molecular properties such as the ionization potential[25,26] of UF_6 have been measured. However, the electron affinity has not been directly determined, even though both experimental and theoretical evidence suggests that its value is relatively high.[27−35] The late Robert Compton was one of the first to study negatively charged UF_6 ions[36] in the gas phase, his studies including its charge transfer reactions and its ion-to-molecule equilibrium. These studies estimated the electron affinity value of UF_6 to lie between 4.9 eV and >5.1 eV.[37] Early theoretical work attributed the high electron affinity of UF_6 to the large formal charge on the uranium center and the nonbonding nature of the orbital into which the electron is captured.[29] Nevertheless, attempts to photodetach electrons from UF_6^- and thus to measure the electron affinity of UF_6 directly were unsuccessful. It was speculated that this was due to a low photodetachment cross section.[35]

In this work, we report the photodetachment of UF_6^- through its anion photoelectron spectrum, thereby further elucidating the electronic structure of UF_6. Importantly, this joint work between experiment and theory provides the first direct determination of the electron affinity of UF_6.

METHODS

Experimental Methods

The details of the anion photoelectron spectrometer used in this work have been described in detail in previous publications.[38] Briefly, anions were generated in an ion source, after which they were directed into a Wiley−McLaren extractor/time-of-flight mass spectrometer (TOFMS) for mass analysis and mass selection. The mass-selected anions of interest were then momentum decelerated to minimize Doppler broadening before entering the anion−photon interaction region, where they intersected perpendicularly with a fixed-frequency laser beam. There, photodetachment occurred, with the resulting electrons being energy-analyzed by a magnetic bottle, time-of-flight electron energy analyzer, these constituting the anion photoelectron spectrometer. The resultant anion photoelectron spectrum (aPES) was calibrated against the known electronic transitions of Au^-.[39] This spectrometer has a resolution of ~50 meV at 1 eV electron kinetic energy (EKE).

Received: April 23, 2026
Revised: June 25, 2026
Accepted: June 29, 2026

The ion source used to generate anions in this study is shown schematically in Figure 1. This source exploits the photoelectric effect,

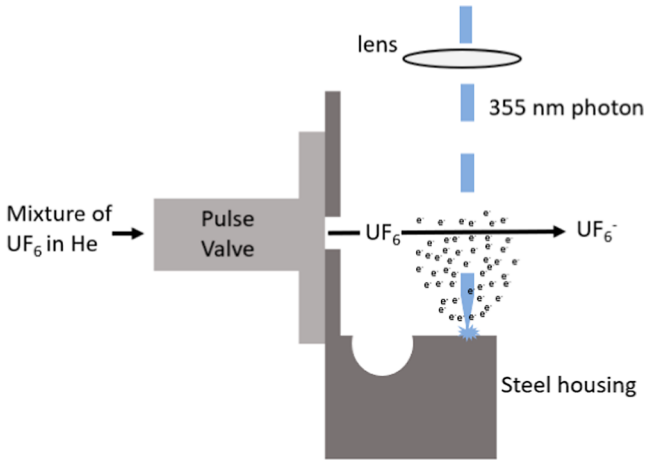

Figure 1. Photoemission anion source. A plume of adiabatically expanded gas containing a mixture of ~0.5−1% depleted UF_6 in He crossed a "shower" of photoemitted electrons from the surface of the steel housing normally used for holding rod.

where light with a photon energy exceeding the work function of a surface is directed onto the surface of the metal, resulting in the emission of low kinetic energy electrons. These electrons then interacted with neutral molecules of UF_6 in an adiabatically expanded gas plume. Typically, to make photoelectrons, we use a rotating and translating metal rod having a low work function. However, in the present work, it was found somewhat serendipitously that high ion intensities of UF_6^- could be generated by focusing light onto the surface of the stainless-steel housing, where a rod would normally be mounted. The resultant "shower" of low-energy electrons then interacted with and attached to the adiabatically expanded plume of 0.5−1% depleted UF_6 vapor seeded in He carrier gas.

Computational Methods

We carried out high-level relativistic coupled-cluster calculations for UF_6^- and UF_6 using the CFOUR program package[40,41] to facilitate the experimental analysis. The equilibrium structures, harmonic vibrational frequencies, and electronic energies of UF_6^- and UF_6 were calculated at the CCSD(T)[42] level using the spin-free exact two-component theory in its one-electron variant (the SFX2C-1e scheme)[43−45] to treat scalar-relativistic effects. To account for the diffuse electron density in the anion, we augmented the SFX2C-1e recontracted Dyall's correlation-consistent polarized valence triple- and quadruple-ζ (dy-pVTZ and dy-pVQZ) basis sets of U,[46] with an additional set of diffuse functions. The exponents of the additional diffuse functions were obtained by multiplying the smallest exponents in each angular momentum by a factor of 0.4. These uranium basis sets are denoted as the dy-apVTZ-X2C and dy-apVQZ-X2C sets. The combination of the dy-apVXZ-X2C sets of U with the aug-cc-pVXZ-X2C sets of F[47] is hereafter referred to as the "AXZ" basis sets.

The equilibrium structures and harmonic vibrational frequencies of UF_6^- and UF_6 were calculated with the ATZ basis sets, using the implementations of analytic gradients for the SFX2C-1e scheme[45] and the CCSD(T)[48] method to expedite the computations. The vertical detachment energy (VDE) of UF_6^- was obtained as the difference between the electronic energies of neutral UF_6 and that of UF_6^- at the equilibrium structure of UF_6^-. The adiabatic electron affinity (AEA) of UF_6 was calculated as the difference between the energies of UF_6^- and UF_6 including zero-point energy (ZPE) corrections obtained within the harmonic approximation. The calculations of VDE and AEA used the ATZ and AQZ basis sets. We then combined the HF/AQZ values with the basis-set-limit electron-correlation contributions obtained from basis-set extrapolation using a two-point formula.[49] The spin−orbit (SO) corrections to the VDE and AEA were obtained as the differences between the equation-of-motion electron attachment coupled-cluster singles and doubles (EOMEA-CCSD)[50,51] calculations using the X2C Hamiltonian[52−54] with atomic mean-field spin−orbit integrals (the X2CAMF scheme)[55−57] and the corresponding SFX2C-1e-EOMEA-CCSD calculations. These X2CAMF calculations used the aug-cc-pVTZ-X2C basis set of F and the X2C spin−orbit contraction[58] for the dy-apVTZ basis set of U.

RESULTS AND DISCUSSION

The mass spectrum obtained under these conditions (Figure 2) shows not only UF_6^-, but also dissociative electron

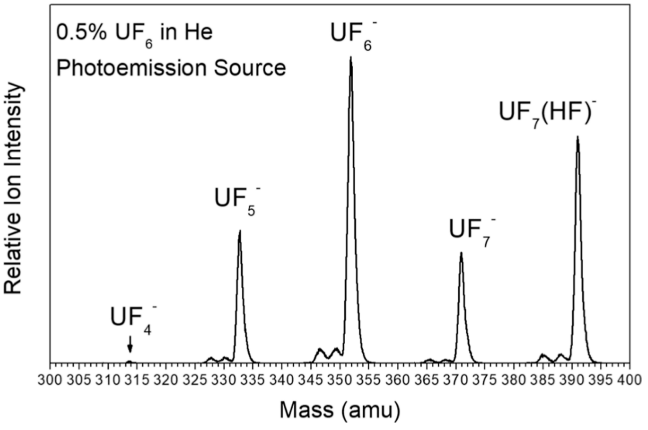

Figure 2. Mass spectrum obtained from a ~0.5% mixture of depleted UF_6 in He from the photoemission ion source shown in Figure 1.

attachment products, with UF_5^- and weak intensities of UF_4^- being observed. A critical factor in generating high intensities of anions from this source was the distance between the axis of the UF_6/He gas plume and the point where the laser beam struck the steel housing, with short distances being optimal.

The measured anion photoelectron spectrum (aPES) of UF_6^- is shown in Figure 3. It was collected with 193 nm (6.42 eV) photons, generated by an excimer laser. The main challenge encountered in acquiring it was the need for the intensity of the photodetached electrons from UF_6^- to be greater than the background electrons (noise) also being generated. The primary source of that background noise was the photoemission of low kinetic energy (EKE) electrons, generated by 193 nm photons striking the walls of the anion−photon interaction region.

The threshold electron binding energy (EBE), corresponding to the onset region of the spectral band in Figure 3, can provide an estimate of the adiabatic electron affinity (AEA) of UF_6. This approximation is valid when the vibrational temperature of the nascent anions is very low, and when the anion and neutral ground state structures are similar enough to afford adequate Franck−Condon overlap. However, since the anions generated in many ion sources are not necessarily cold, the resulting anions may exhibit vibrational hot bands, i.e., photodetachment from vibrationally excited negative ions. These hot bands can contribute to low-EBE features in the spectrum, complicating the assignment of the true spectral origin. Still, one can estimate the location of the spectral origin of the spectrum, which corresponds to the AEA value, by locating a significant change in the slope of the photoelectron

https://doi.org/10.1021/jacs.6c08451
J. Am. Chem. Soc. XXXX, XXX, XXX−XXX

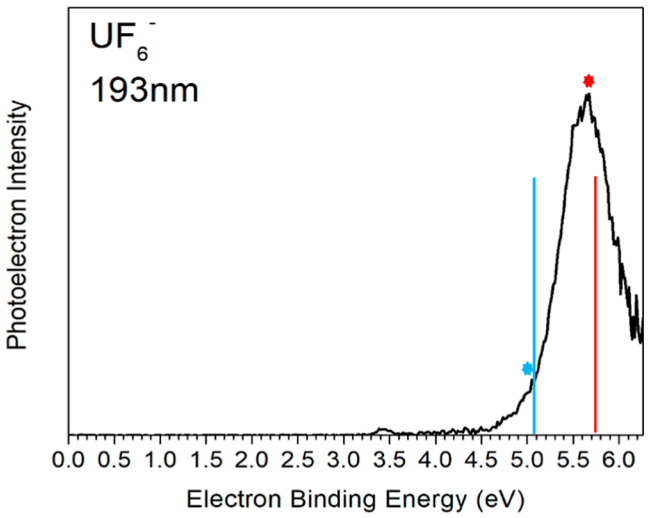

Figure 3. Anion photoelectron spectrum of UF_6^- measured with 193 nm (6.42 eV) photons. The red star and the red stick mark the experimentally determined VDE value (5.66 eV) and the calculated relativistic coupled-cluster VDE value (5.73 eV) for UF_6^-, respectively. The blue star and the blue stick mark to the experimental (5.05 eV) and computational (5.09 eV) AEA values of UF_6, respectively. Note the small peak at EBE = 3.40 eV. It is due to a two-photon process, i.e., the photodissociation of $UF_6^- \rightarrow UF_5 + F^-$, followed by the photodetachment of F^-. The EA of F is 3.40 eV.

intensity "tail" and/or by extrapolating the low EBE side of the main spectral band.

In contrast, the vertical detachment energy (VDE) of an anion is more definitively determined since it corresponds to the maximum overlap of the vibronic wave functions of the anion's ground state to that of its corresponding neutral at the anion's equilibrium geometry. It is a vertical transition. As such, the VDE appears as the most intense low EBE peak in the anion photoelectron spectrum. Thus, the VDE of UF_6^- is 5.66 ± 0.10 eV. Accordingly, the EBE that corresponds to the AEA value lies between the threshold of the spectrum at EBE ∼ 4.6 eV and the VDE of UF_6^- at 5.66 eV. Based on the spectrum, the AEA value is estimated to be 5.05 ± 0.10 eV, consistent with the calculated AEA value of 5.09 eV.

Neutral UF_6 is a closed-shell molecule, whereas the additional electron in the radical anion UF_6^- is situated on a uranium 5f orbital (Figure 4). The repulsion between this open-shell, nonbonding electron and the electron density in the U−F bonds significantly increases the U−F bond lengths. The U−F bond length in UF_6^- is about 0.08 Å longer than that in UF_6 (Table 1). Accordingly, the vibrational frequencies of the U−F stretching modes in UF_6^- are substantially lower than those in UF_6. For example, the harmonic frequency for the t_{1u} mode is reduced by 85 cm^{-1} in the presence of this additional electron in UF_6^- (Table 1). The large difference in the U−F bond lengths in UF_6^- and UF_6 is consistent with the significant (unresolved) vibrational progression in the anion photoelectron spectrum of UF_6^-.

As summarized in Table 2, the basis-set contributions beyond the triple-ζ ATZ basis amount to 0.13 eV for VDE and 0.04 eV for AEA. The SO correction is around 0.1 eV for both VDE and AEA. With the inclusion of basis-set contributions, the SO corrections, and zero-point energy corrections, the computed VDE of 5.73 eV and AEA of 5.09 eV are in good agreement with the measured spectral features; they seem to

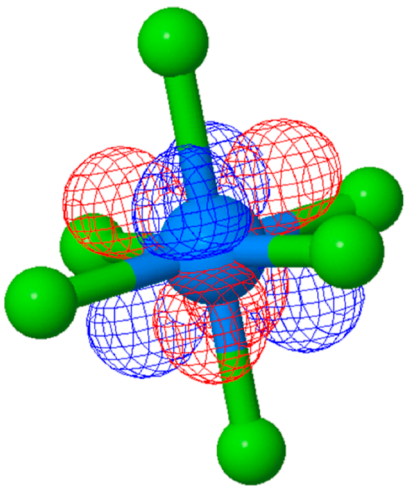

Figure 4. A_{2u} molecular orbital of the unpaired electron in the electronic ground state of the UF_6^- anion. It mainly consists of contributions from a uranium 5f orbital.

Table 1. SFX2C-1e-CCSD(T)/ATZ U−F Bond Lengths (Å) and Harmonic Vibrational Frequencies (cm^{-1}) for the U−F Stretching Modes in UF_6^- and UF_6

	UF_6^-	UF_6
R [U−F] (Å)	2.079	2.000
ω_e [U−F, a_{1g}] (cm^{-1})	655	686
ω_e [U−F, t_{1u}] (cm^{-1})	546	631
ω_e [U−F, e_g] (cm^{-1})	466	539

Table 2. SFX2C-1e-CCSD(T) Vertical Detachment Energy Values for UF_6^- and Adiabatic Electron Affinity Values for UF_6 Augmented with Spin−Orbit Corrections and Zero-Point Energy Corrections

unit: eV	VDE	AEA
ATZ	5.47	4.93
AQZ	5.54	4.95
∞Z	5.60	4.97
$+\Delta_{SO}$	5.73	5.07
$+\Delta_{vib}$	--	5.09
measured	5.66	5.05

slightly overestimate the measured values. The computed VDE is around 0.6 eV higher than the computed AEA value, which is consistent with the width of the observed spectral band (due to the unresolved vibrational progression) in the anion photoelectron spectrum. These high-level *ab initio* calculations provide definitive support for the assignment of the measured spectral features in the anion photoelectron spectrum of UF_6^-. The measurement provides benchmark results that confirm that the DFT results in ref 35 substantially underestimate the electron affinity of $UF6^-$. The CCSD(T) results for VDE and AEA in ref 35 qualitatively agree with the measurement and our calculations, but exhibits larger errors mainly due to the small basis sets.

CONCLUSION

We report a joint anion photoelectron spectroscopic and *ab initio* computational study of the photodetachment of the uranium hexafluoride anion (UF_6^-). High-level relativistic coupled-cluster calculations, incorporating rigorous treatments

https://doi.org/10.1021/jacs.6c08451
J. Am. Chem. Soc. XXXX, XXX, XXX−XXX

of scalar-relativistic, spin−orbit, and basis-set effects, predict the vertical detachment energy (VDE) of UF_6^- and the adiabatic electron affinity (AEA) of UF_6 to be in excellent agreement with the measured anion photoelectron spectrum. The synergy between experiment and computation provides definitive support for assigning the observed spectral features to the photodetachment of UF_6^- to neutral UF_6, a molecule of importance in nuclear energy science. The photodetachment process involves removal of an electron from a uranium 5f orbital, with the AEA of UF_6 and VDE of UF_6^- determined to be 5.05 and 5.66 eV, respectively.

■ ASSOCIATED CONTENT

Supporting Information

The Supporting Information is available free of charge at https://pubs.acs.org/doi/10.1021/jacs.6c08451.

The Supporting Information contains the SFX2C-1e recontracted uranium and fluorine Dyall's basis sets used in the relativistic electronic structure calculations, provided in the CFOUR format (PDF)

■ AUTHOR INFORMATION

Corresponding Authors

Lan Cheng − *Department of Chemistry, The Johns Hopkins University, Baltimore, Maryland 21218, United States;* orcid.org/0000-0003-1165-9559; Email: lcheng24@jhu.edu

Kit H. Bowen − *Department of Chemistry, The Johns Hopkins University, Baltimore, Maryland 21218, United States;* orcid.org/0000-0002-2858-6352; Email: kbowen@jhu.edu

Authors

Burak A. Tufekci − *Department of Chemistry, The Johns Hopkins University, Baltimore, Maryland 21218, United States;* orcid.org/0000-0002-6964-6630

Shiying Wang − *Department of Chemistry, The Johns Hopkins University, Baltimore, Maryland 21218, United States;* orcid.org/0009-0007-6318-8580

Complete contact information is available at: https://pubs.acs.org/10.1021/jacs.6c08451

Notes

The authors declare no competing financial interest.

■ ACKNOWLEDGMENTS

The experimental material in this work was supported by the Heavy Elements Chemistry (HEC) program of the Department of Energy (DOE) under grant number, DE-SC0022977 (K.H.B.). Numerous inspiring conversations with R.N. Compton about UF_6 are acknowledged by K.H.B. The computational material in this work was supported by the Department of Energy Early Career Research Program under Award Number DE-SC0020317 (L.C.). The computations at Johns Hopkins University were carried out at Advanced Research Computing at Hopkins (ARCH) core facility (rockfish.jhu.edu), which is supported by the National Science Foundation (NSF) under grant number OAC-1920103.

■ REFERENCES

(1) Grosse, A. V. *Chemical Properties of Uranium Hexafluoride, UF6*; Columbia University, 1941; Vol. *A-83*, 962915.

(2) Katz, J. J.; Rabinowitch, E. The Chemistry of Uranium The Element, Its Binary and Related Compounds. In *National Nuclear Energy Series*; Dover Publications, 1951; Vol. *5*.

(3) Morss, L. R.; Edelstein, N. M.; Fuger, J. *The Chemistry of the Actinide and Transactinide Elements; Springerlink BüCher*; Springer Netherlands: Dordrecht, 2011.

(4) Glasstone, S.; Sesonske, A. *Nuclear Reactor Engineering*, 3rd ed.; Van Nostrand Reinhold: New York, 1981.

(5) Goldwhite, H. The Manhattan Project. *J. Fluor. Chem.* **1986**, *33* (1−4), 109−132.

(6) Becker, F. S.; Kompa, K. L. The Practical and Physical Aspect of Uranium Isotope Separation with Lasers. *Nucl. Technol.* **1982**, *58* (2), 329−353.

(7) Takeuchi, K.; Tashiro, H.; Kato, S.; Midorikawa, K.; Oyama, T.; Satooka, S.; Namba, S. Infrared Multiphoton Dissociation of UF_6 in Supersonic Nozzle Reactor. *J. Nucl. Sci. Technol.* **1989**, *26* (2), 301−303.

(8) Baranov, V. Y.; Kolesnikov, Y. A.; Kotov, A. A. Laser Photolysis of UF_6 Molecules. *Quantum Electron.* **1999**, *29* (8), 653−666.

(9) Makarov, G. N. Towards Molecular Laser Separation of Uranium Isotopes. *Usp. Fiz. Nauk* **2022**, *65* (06), 531−566.

(10) Kuga, Y.; Endoh, S.; Satooka, S.; Okada, Y.; Tashiro, H.; Takeuchi, K. Collection of^{235} U-Enriched UF_5 Particles and Direct Measurement of Separation Factor in Laser Isotope Separation of Uranium. *J. Nucl. Sci. Technol.* **1991**, *28* (9), 870−872.

(11) Okada, Y.; Kato, S.; Satooka, S.; Tashiro, H.; Takeuchi, K. An Apparatus for Isotopic Ratio Measurement in UF_5 Formed by Infrared Multiphoton Dissociation of UF_6 in Molecular Beam. *J. Nucl. Sci. Technol.* **1995**, *32* (11), 1174−1180.

(12) Heaven, M. C.; Gibson, J. K.; Marçalo, J. Molecular Spectroscopy and Reactions of Actinides in the Gas Phase and Cryogenic Matrices. In *The Chemistry of the Actinide and Transactinide Elements*; Morss, L. R., Edelstein, N. M., Fuger, J., Eds.; Springer Netherlands: Dordrecht, 2010; pp 4079−4156.

(13) Seppelt, K. Molecular Hexafluorides. *Chem. Rev.* **2015**, *115* (2), 1296−1306.

(14) Kim, K. C.; Mulford, R. N. Vibrational Properties of Actinide (U, Np, Pu, Am) Hexafluoride Molecules. *J. Mol. Struct. THEOCHEM* **1990**, *207* (3−4), 293−299.

(15) Frlec, B.; Claassen, H. H. Long-Wavelength, Infrared-Active Fundamental for Uranium, Neptunium, and Plutonium Hexafluorides. *J. Chem. Phys.* **1967**, *46* (12), 4603−4604.

(16) Aldridge, J. P.; Brock, E. G.; Filip, H.; Flicker, H.; Fox, K.; Galbraith, H. W.; Holland, R. F.; Kim, K. C.; Krohn, B. J.; Magnuson, D. W.; Maier, W. B.; McDowell, R. S.; Patterson, C. W.; Person, W. B.; Smith, D. F.; Werner, G. K. Measurement and Analysis of the Infrared-Active Stretching Fundamental (N3) of UF6. *J. Chem. Phys.* **1985**, *83* (1), 34−48.

(17) Paine, R. T.; McDowell, R. S.; Asprey, L. B.; Jones, L. H. Vibrational Spectroscopy of Matrix-Isolated UF6 and UF5. *J. Chem. Phys.* **1976**, *64* (7), 3081−3083.

(18) Holland, R. F.; Maier, W. B. Absorption in the ν_3 Band of UF_6 Dissolved in Solid Xenon. *Spectrosc. Lett.* **1983**, *16* (6), 409−412.

(19) Myerson, A. L.; Chludzinski, J. J. Chemical Kinetics of the Gas-Phase Reaction between Uranium Hexafluoride and Hydrogen. *J. Phys. Chem.* **1981**, *85* (25), 3905−3911.

(20) Straka, M.; Patzschke, M.; Pyykk, P. Why Are Hexavalent Uranium Cyanides Rare While U?F and U?O Bonds Are Common and Short? *Theor. Chem. Acc. Theory Comput. Model. Theor. Chim. Acta* **2003**, *109* (6), 332−340.

(21) Onoe, J.; Takeuchi, K.; Nakamatsu, H.; Mukoyama, T.; Sekine, R.; Kim, B.-I.; Adachi, H. Relativistic Effects on the Electronic Structure and Chemical Bonding of UF6. *J. Chem. Phys.* **1993**, *99* (9), 6810−6817.

(22) Graubner, T.; Karttunen, A. J.; Kraus, F. A Computational Study on Closed-Shell Molecular Hexafluorides M F_6 (M = S, Se, Te,

Po, Xe, Rn, Cr, Mo, W, U) − Molecular Structure, Anharmonic Frequency Calculations, and Prediction of the NdF_6 Molecule. *ChemPhysChem* **2023**, *24* (9), No. e202200903.
(23) Denning, R. G. Electronic Structure and Bonding in Actinyl Ions and Their Analogs. *J. Phys. Chem. A* **2007**, *111* (20), 4125−4143.
(24) Büyükmumcu, Z.; Selampinar, F. Revisiting UF6, NpF6 and PuF6 for Bonding and Molecular Surface Analysis within Density Functional Theory: Comparative Study at the Different Theory Levels with the Same Basis Set. *Polyhedron* **2021**, *209*, 115452.
(25) Hildenbrand, D. L. Thermochemistry of Gaseous UF5 and UF4. *J. Chem. Phys.* **1977**, *66* (11), 4788−4794.
(26) Potts, A. W.; Lempka, H. J.; Streets, D. G.; Price, W. C. Photoelectron Spectra of the Halides of Elements in Groups III, IV, V and VI. *Philos. Trans. R. Soc. London Ser. Math. Phys. Sci.* **1970**, *268* (1184), 59.
(27) Sidorov, L. N. Molecules with a High Electron Affinity. *Russ. Chem. Rev.* **1982**, *51* (4), 356−367.
(28) Boring, M.; Wood, J. H. Relativistic Calculation of the Electronic Structure of UF6. *J. Chem. Phys.* **1979**, *71* (1), 32−41.
(29) Hay, P. J.; Wadt, W. R.; Kahn, L. R.; Raffenetti, R. C.; Phillips, D. H. A b i n i t i o Studies of the Electronic Structrue of UF6, UF6+, and UF−6 Using Relativistic Effective Core Potentials. *J. Chem. Phys.* **1979**, *71* (4), 1767−1779.
(30) Armstrong, D. P.; Harkins, D. A.; Compton, R. N.; Ding, D. Multiphoton Ionization of Uranium Hexafluoride. *J. Chem. Phys.* **1994**, *100* (1), 28−43.
(31) Beauchamp, J. L. Ion Cyclotron Resonance Studies of Endothermic Reactions of UF−6 Generated by Surface Ionization. *J. Chem. Phys.* **1976**, *64* (3), 929−935.
(32) Dittner, P. F.; Datz, S. Molecular Negative Surface Ionization of UF6. *J. Chem. Phys.* **1978**, *68* (5), 2451−2456.
(33) Borshchevskii, A. Y.; Boltalina, O. V.; Sorokin, I. D.; Sidorov, L. N. Thermochemical Quantities for Gas-Phase Iron, Uranium, and Molybdenum Fluorides, and Their Negative Ions. *J. Chem. Thermodyn.* **1988**, *20* (5), 523−537.
(34) Skokan, E. V.; Sorokin, I. D.; Nikitin, M. I.; Chilingarov, N. S.; Sidorov, L. N. *The Electron Affinity of Uranium Hexafluoride*; International Atomic Energy Agency, 1983; Vol. *57*, p 1745.
(35) Dau, P. D.; Su, J.; Liu, H.-T.; Huang, D.-L.; Wei, F.; Li, J.; Wang, L.-S. Photoelectron Spectroscopy and Theoretical Studies of UF5− and UF6. *J. Chem. Phys.* **2012**, *136* (19), 194304.
(36) Stockdale, J. A. D.; Compton, R. N.; Schweinler, H. C. Negative Ion Formation in Selected Hexafluoride Molecules. *J. Chem. Phys.* **1970**, *53* (4), 1502−1507.
(37) Compton, R. N. On the Formation of Positive and Negative Ions in Gaseous UF6. *J. Chem. Phys.* **1977**, *66* (10), 4478−4485.
(38) Marshall, M.; Zhu, Z.; Harris, R.; Collins, E.; Bowen, K. H. Photoelectron Spectroscopic Study of Ascorbate and Deprotonated Ascorbate Anions Using an Electrospray Ion Source and a Cryogenically Cooled Ion Trap. *J. Phys. Chem. A* **2021**, *125* (35), 7699−7704.
(39) Ho, J.; Ervin, K. M.; Lineberger, W. C. Photoelectron Spectroscopy of Metal Cluster Anions: Cu− n, Ag− n, and Au− n. *J. Chem. Phys.* **1990**, *93* (10), 6987−7002.
(40) Matthews, D. A.; Cheng, L.; Harding, M. E.; Lipparini, F.; Stopkowicz, S.; Jagau, T.-C.; Szalay, P. G.; Gauss, J.; Stanton, J. F. Coupled-Cluster Techniques for Computational Chemistry: The CFOUR Program Package. *J. Chem. Phys.* **2020**, *152* (21), 214108.
(41) Stanton, J. F.; Gauss, J.; Cheng, L.; Harding, M. E.; Matthews, D. A.; Lipparini, F.; Szalay, P. G.; Stopkowicz, S. C. F. O. U. R.. *Coupled-Cluster Techniques for Computational Chemistry, a Quantum-Chemical Program Package*, 2023; Vol. *32*.
(42) Raghavachari, K.; Trucks, G. W.; Pople, J. A.; Head-Gordon, M. A Fifth-Order Perturbation Comparison of Electron Correlation Theories. *Chem. Phys. Lett.* **1989**, *157* (6), 479−483.
(43) Dyall, K. G. Interfacing Relativistic and Nonrelativistic Methods. IV. One- and Two-Electron Scalar Approximations. *J. Chem. Phys.* **2001**, *115* (20), 9136−9143.
(44) Liu, W.; Peng, D. Exact Two-Component Hamiltonians Revisited. *J. Chem. Phys.* **2009**, *131* (3), 031104.
(45) Cheng, L.; Gauss, J. Analytic Energy Gradients for the Spin-Free Exact Two-Component Theory Using an Exact Block Diagonalization for the One-Electron Dirac Hamiltonian. *J. Chem. Phys.* **2011**, *135* (8), 084114.
(46) Dyall, K. G. Relativistic Double-Zeta, Triple-Zeta, and Quadruple-Zeta Basis Sets for the Actinides Ac−Lr. *Theor. Chem. Acc.* **2007**, *117* (4), 491−500.
(47) Dunning, T. H. Gaussian Basis Sets for Use in Correlated Molecular Calculations. I. The Atoms Boron through Neon and Hydrogen. *J. Chem. Phys.* **1989**, *90* (2), 1007−1023.
(48) Watts, J. D.; Gauss, J.; Bartlett, R. J. Open-Shell Analytical Energy Gradients for Triple Excitation Many-Body, Coupled-Cluster Methods: MBPT(4), CCSD+T(CCSD), CCSD(T),and QCISD(T). *Chem. Phys. Lett.* **1992**, *200* (1−2), 1−7.
(49) Helgaker, T.; Klopper, W.; Koch, H.; Noga, J. Basis-Set Convergence of Correlated Calculations on Water. *J. Chem. Phys.* **1997**, *106* (23), 9639−9646.
(50) Stanton, J. F.; Bartlett, R. J. The Equation of Motion Coupled-Cluster Method. A Systematic Biorthogonal Approach to Molecular Excitation Energies, Transition Probabilities, and Excited State Properties. *J. Chem. Phys.* **1993**, *98* (9), 7029−7039.
(51) Nooijen, M.; Bartlett, R. J. Equation of Motion Coupled Cluster Method for Electron Attachment. *J. Chem. Phys.* **1995**, *102* (9), 3629−3647.
(52) Dyall, K. G. Interfacing Relativistic and Nonrelativistic Methods. I. Normalized Elimination of the Small Component in the Modified Dirac Equation. *J. Chem. Phys.* **1997**, *106* (23), 9618−9626.
(53) Kutzelnigg, W.; Liu, W. Quasirelativistic Theory Equivalent to Fully Relativistic Theory. *J. Chem. Phys.* **2005**, *123* (24), 241102.
(54) Iliaš, M.; Saue, T. An Infinite-Order Two-Component Relativistic Hamiltonian by a Simple One-Step Transformation. *J. Chem. Phys.* **2007**, *126* (6), 064102.
(55) Liu, J.; Cheng, L. An Atomic Mean-Field Spin-Orbit Approach within Exact Two-Component Theory for a Non-Perturbative Treatment of Spin-Orbit Coupling. *J. Chem. Phys.* **2018**, *148* (14), 144108.
(56) Zhang, C.; Cheng, L. Atomic Mean-Field Approach within Exact Two-Component Theory Based on the Dirac−Coulomb−Breit Hamiltonian. *J. Phys. Chem. A* **2022**, *126* (27), 4537−4553.
(57) Asthana, A.; Liu, J.; Cheng, L. Exact Two-Component Equation-of-Motion Coupled-Cluster Singles and Doubles Method Using Atomic Mean-Field Spin-Orbit Integrals. *J. Chem. Phys.* **2019**, *150* (7), 074102.
(58) Zhang, C.; Peterson, K. A.; Dyall, K. G.; Cheng, L. A New Computational Framework for Spinor-Based Relativistic Exact Two-Component Calculations Using Contracted Basis Functions. *J. Chem. Phys.* **2024**, *161* (5), 054105.

https://doi.org/10.1021/jacs.6c08451
J. Am. Chem. Soc. XXXX, XXX, XXX−XXX